

Averaged Value Analysis of 24-Pulse Rectifiers for Aerospace Applications

Sakineh Aghighi

Department of Electrical Engineering
Jihad University Institute of Higher Education
Unit of Hamedan
Hamedan, IRAN
zohreh.aghighi@gmail.com

Reza Ebrahimi Atani

Department of Electrical Engineering
The University of Guilan
P.O. Box 3756, Rasht, IRAN
rebrahimi@guilan.ac.ir

Abstract—This paper presents a new average modeling approach for 24-pulse rectifiers. The model is based on the former non-linear averaged value models for different configurations of an 24-pulse rectifier. The models allow rectifier and drive system interactions to be examined analytically, or through rapid simulation. The models are validated by comparison with a detailed circuit simulation.

I. INTRODUCTION

Multi-pulse transformer based or autotransformer based diode rectifiers are usually used as front end converter in aerospace applications. Compared to PWM active front end converters, multi-pulse diode rectifiers are lighter, more reliable, and in all represent a much lower cost solution. For power system integration however, their switching action is still a hindrance for system simulation, impedance measurements, and AC and DC stability studies. For this reason, the usage and development of average models has become a powerful system design tool for aerospace applications, since this type of model averages out the switching action of power converters, rendering their software simulation models continuous and hence ready for linearization and small-signal analyses. Due to their internal control functions, power electronic converters present 'constant power' characteristics to their supply. These types of loads are known as Constant Power Loads (CPLs). Since CPLs have negative incremental input impedance, there is a possibility of interaction, lightly damped oscillations and instability between the supply and the CPL, or between different CPLs sinking energy from one supply. This instability issue has led to the need for more thorough analysis of systems which are composed of multi-CPLs.

Over the past few years, there has been a significant amount of research on DC power distribution systems which contain tightly regulated converters. However, there are only a few papers published about AC systems which consist of rectifiers and constant power loads [2]. Using standard circuit simulation techniques to study the dynamic interaction between a single rectifier, DC link and CPL can be very demanding computationally due to the large number of diode commutations that must be calculated in a typical transient. As an alternative, averaged-value, DC-side models of the rectifier may be used. The dynamics of the resultant

equivalent circuit may be either studied analytically, or used in a circuit simulator to reduce simulation times substantially. While the literature shows that averaged models of 6-pulse bridge rectifiers have been developed which are suitable for small signal analysis, ([3], [4], [5]) there are only a few works on the averaged models of multi-pulse rectifiers. In [6] and [8] averaged value analysis of 12-Pulse and 18-pulse rectifiers have already been carefully studied.

The main goal of this paper is to present a new average modeling approach for 24-pulse rectifiers. The modeling is simulated for different configurations of an 24-pulse rectifier. The model is based on the former non-linear averaged value models for different configurations of an 24-pulse rectifier. This model has already been used for 12-pulse [6] and 18-pulse [8] rectifiers. The models allow rectifier and drive system interactions to be examined analytically, or through rapid simulation. To validate the averaged models of the rectifiers, the results from the equivalent circuits are compared with those from detailed circuit simulations undertaken in Micro-Cap SPICE. The Micro-Cap simulation model used ideal diodes and lossless components. The transformer and autotransformer magnetising inductances were set to very high values, resulting in negligible magnetising current. A constant power load was used in the simulations and a large signal step change in load power was used to assess the models. The operation of 24-pulse converter results in the absence of the 17th and 19th harmonics in the input utility line current, and also increases the stability of the system.

The rest of the paper is structured as follows: a general description of the averaged model of a general 24-pulse rectifier is presented in section II. Section III describes the averaged value model of alternative 24-pulse rectifiers. Comparison of models is in section IV and the paper concludes in section V.

II. AVERAGED VALUE MODEL OF A GENERAL 24-PULSE RECTIFIER

In this section we will describe the average value model of a generic 24-pulse rectifier. Figure 1 shows the schematic diagram of a general 24-pulse rectifier. The AC power supply is assumed to consist of three ideal, balanced voltage sources

with 120° phase difference and three line inductors. The line-to-neutral voltages are expressed by the vector of v_s :

$$v_s = \begin{bmatrix} V_A \\ V_B \\ V_C \end{bmatrix} = V_m \cdot \begin{bmatrix} \cos(\omega t) \\ \cos(\omega t - 2\pi/3) \\ \cos(\omega t + 2\pi/3) \end{bmatrix} \quad (1)$$

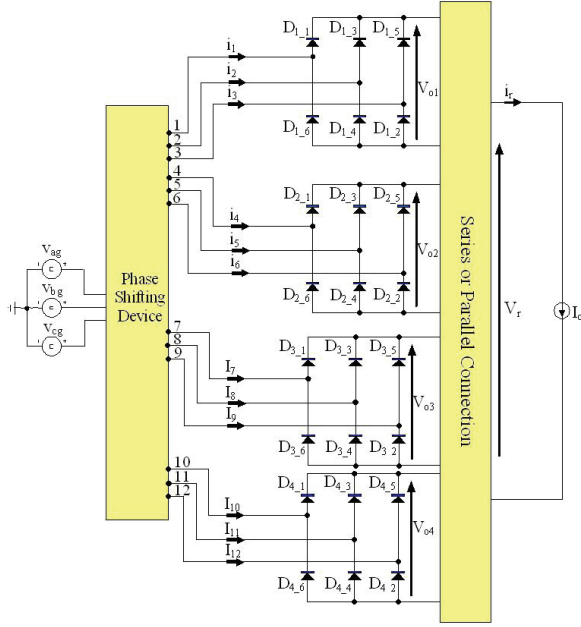


Fig. 1. A Generic 24-pulse rectifier

The transformer is a three-phase transformer with three three-phase output voltages, which have the same amplitude, and there is a 15° phase shift between them. The four six-pulse rectifiers are connected in series or parallel to feed a constant power load via a second-order DC link filter. The four equal inductors $L_{p1} = L_{p2} = L_{p3} = L_{p4} = L_p$ represent the primary leakage inductances and the inductance of the supply lines. The inductors $L_{s1} = L_{s2} = L_{s3} = L_{s4} = L_s$ represent the transformer secondary leakage series inductances. The forward resistance of the diodes and the resistance of the DC link inductor are included. The model is derived by averaging the state variables across each 15° portion of the supply waveform. Each 15° portion begins with an overlap transient as the DC link current commutates between diodes, whilst in the second part of the 15° interval only two diodes in each bridge are in conduction. A straight line is assumed between initial and final values of every phase current.

The output voltages of the 6 pulse rectifiers are V_1 , V_2 , V_3 and V_4 . The matrix equations of them are:

$$\begin{bmatrix} V_1 \\ V_2 \\ V_3 \\ V_4 \end{bmatrix} = A v_s - B \frac{d}{dt}(i_1) - C \frac{d}{dt}(i_2) - D \frac{d}{dt}(i_3) - E \frac{d}{dt}(i_4) \quad (2)$$

Where i_1 , i_2 , i_3 and i_4 are vectors of the line currents of each rectifier.

$$i_1 = [I_1, I_2, I_3]^T \quad (3)$$

$$i_2 = [I_4, I_5, I_6]^T \quad (4)$$

$$i_3 = [I_7, I_8, I_9]^T \quad (5)$$

$$i_4 = [I_{10}, I_{11}, I_{12}]^T \quad (6)$$

The matrixes A , B , C , D , and E , are coefficient matrixes and the values of them depend on the type of three-phase transformer and the system analysis interval and can be easily obtained as described in [13].

The rectifier output voltage equation is obtained by summation of V_1 , V_2 , V_3 , and V_4 for serial configuration. However, for parallel configuration, because of the interphase reactor(s), the output voltage is average of V_1 , V_2 , V_3 , and V_4 and the effect of interphase reactor leakage inductance(s) will appear as an inductance in series with the rest of the circuit. Therefore a general equation for \bar{V}_r is:

$$\bar{V}_r = A \cdot v_s - B \frac{d}{dt}(i_1) - C \frac{d}{dt}(i_2) - D \frac{d}{dt}(i_3) - E \frac{d}{dt}(i_4) - F \frac{d}{dt}(i_L) \quad (7)$$

Where i_L is the DC load current. The matrixes A , B , C , D and E are also the coefficient matrixes, and as it is mentioned before the values of them depend on the three-phase transformer and the system analysis interval and the matrix F depends on the connection type of bridge's outputs and the number of interphase reactors.

The average output voltage of \bar{V}_r is determined by integrating 7 over one of its switching intervals, which is 15° and it is between $\theta_1 < t < \theta_2$.

$$\begin{aligned} \bar{V}_r &= \frac{1}{\pi/12} \int_{\theta_1}^{\theta_2} (A v_s) d\theta - B \frac{[i_1(\theta_2) - i_1(\theta_1)]}{\Delta t} - C \frac{[i_2(\theta_2) - i_2(\theta_1)]}{\Delta t} \\ &- D \frac{[i_3(\theta_2) - i_3(\theta_1)]}{\Delta t} - E \frac{[i_4(\theta_2) - i_4(\theta_1)]}{\Delta t} - F \frac{d}{dt}(i_L) \end{aligned} \quad (8)$$

$$\begin{aligned} \bar{V}_r &= \frac{1}{\pi/12} \int_{\theta_1}^{\theta_2} (A v_s) d\theta - \frac{12\omega}{\pi} B \begin{bmatrix} -i \\ -\Delta i \\ \Delta i \end{bmatrix} - \frac{12\omega}{\pi} C \begin{bmatrix} -\Delta i \\ i + \Delta i \\ \Delta i \end{bmatrix} \\ &- \frac{12\omega}{\pi} D \begin{bmatrix} -\Delta i \\ i + \Delta i \\ 0 \end{bmatrix} - \frac{12\omega}{\pi} E \begin{bmatrix} -i \\ i + \Delta i \\ -\Delta i \end{bmatrix} - F \frac{d}{dt}(i_L) \end{aligned} \quad (9)$$

Where $\Delta t = \frac{\pi}{12\omega}$ and $\frac{d}{dt}(i_L)$ is the local rate of change of the DC-link current. It is assumed the DC load current is i_L at the beginning of this time interval and there is a small linear Δi change at the end of it. Δi denotes the change in average current over $\frac{\pi}{12}$ period and is approximated as $\Delta i \approx \frac{di}{dt} \cdot \Delta t = \frac{\pi}{12\omega} \frac{di}{dt}$. The current values of the bridge lines at this interval are the same for every configuration if the conducting interval is chosen in that manner which it starts at θ_1 when a current transfer is started from $D1 - 1$ to $D1 - 4$, and finishes at θ_2 when a current transfer is started from $D4 - 2$ to $D4 - 6$.

The averaged output voltage of every configuration is attainment by substituting the values of Table 1 into integration

TABLE I
THE VALUES OF LINES CURRENT OF TWO BRIDGES AT THE $\theta_1 < \alpha < \theta_2$
INTERVAL

	θ_1	θ_2
$I(L_1)$	$-i$	0
$I(L_2)$	$-i$	$-i - \Delta i$
$I(L_3)$	i	$i + \Delta i$
$I(L_4)$	$-i$	$-i - \Delta i$
$I(L_5)$	0	$i + \Delta i$
$I(L_6)$	i	$i + \Delta i$
$I(L_7)$	$-i$	$-i - \Delta i$
$I(L_8)$	0	$i + \Delta i$
$I(L_9)$	0	0
$I(L_{10})$	i	0
$I(L_{11})$	0	$i + \Delta i$
$I(L_{12})$	$-i$	$-i - \Delta i$

of (9) and simplifying.

$$\begin{aligned} \overline{V}_r &= \frac{1}{\pi/12} \int_{\theta_1}^{\theta_2} (Av_s) d\theta - \frac{12\omega}{\pi} B \left[-\frac{i}{12\omega} \frac{di_r}{dt} \right] \\ &- \frac{12\omega}{\pi} C \left[\begin{array}{c} -\frac{\pi}{12\omega} \frac{di_r}{dt} \\ i + \frac{\pi}{12\omega} \frac{di_r}{dt} \\ \frac{\pi}{12\omega} \frac{di_r}{dt} \end{array} \right] - \frac{12\omega}{\pi} D \left[\begin{array}{c} -\frac{\pi}{12\omega} \frac{di_r}{dt} \\ i + \frac{\pi}{12\omega} \frac{di_r}{dt} \\ 0 \end{array} \right] \\ &- \frac{12\omega}{\pi} E \left[\begin{array}{c} -i \\ i + \frac{\pi}{12\omega} \frac{di_r}{dt} \\ -\frac{\pi}{12\omega} \frac{di_r}{dt} \end{array} \right] - F \frac{d}{dt}(i_L) \end{aligned} \quad (10)$$

$$\begin{aligned} \overline{V}_r &= \frac{12\omega}{\pi} A \int_{\theta_1/\omega}^{\theta_2/\omega} v_s dt - \left(k_0 r B \begin{bmatrix} 0 \\ -1 \\ 1 \end{bmatrix} + k_0 r C \begin{bmatrix} -1 \\ 1 \\ 1 \end{bmatrix} \right) \\ &- \frac{12\omega}{\pi} \left(k_0 L(B) \begin{bmatrix} -1 \\ 0 \\ 0 \end{bmatrix} + k_0 L(C) \begin{bmatrix} 0 \\ 1 \\ 0 \end{bmatrix} \right) \overline{i}_r \\ &- \left(k_0 L \left(D \begin{bmatrix} 0 \\ 1 \\ 0 \end{bmatrix} + E \begin{bmatrix} -1 \\ 1 \\ 0 \end{bmatrix} \right) \right) \overline{i}_r + \\ &- \left(k_0 r \left(D \begin{bmatrix} -1 \\ 1 \\ 0 \end{bmatrix} + E \begin{bmatrix} 0 \\ 1 \\ -1 \end{bmatrix} \right) \right) \frac{d\overline{i}_r}{dt} \end{aligned} \quad (11)$$

The values of A , B , C , D , E and F depend on the configurations. Note that for series connections $k_0 = 1$ and for parallel connections, $k_0 = 0.25$.

III. AVERAGED VALUE MODEL OF ALTERNATIVE 24-PULSE RECTIFIERS

A. Serie Y/ZYZΔ connection

When a Y/ZYZΔ transformer is used as the phase shifting device, the values of θ_1 , and θ_2 are $9\pi/24$ and $13\pi/24$ respectively for the 15° interval that starts with the commutation from D1-1 to D1-4. In a series connection an inter-phase reactor is not required, so the constant $k_0 = 1$ and $G = 0$. The expressions for the terms in equation (11) are listed in table II. Substituting these values into (11) will lead us to \overline{V}_r :

$$\begin{aligned} \overline{V}_r &= \frac{12\sqrt{3.267}nVm}{\pi} - [12.3(0.36 + \frac{\sqrt{3.267}}{2})n^2L_p + \\ &2.36(1.82 + \frac{\sqrt{3.267}}{2})n^2L_s + 12L_s] \frac{d\overline{i}_r}{dt} - \\ &[\frac{12\omega n^2(0.82L_p + 0.36L_s)(3.267L_p + 0.27L_s)}{\pi} \left(0.36 + \frac{\sqrt{3.267}}{2} \right) + \\ &9.267n^2r_p \left(1 + \frac{\sqrt{3.267}}{2} \right) + 9.36n^2r_s + 9.36r_s] \overline{i}_r \end{aligned} \quad (12)$$

TABLE II
REQUIRED PARAMETERS FOR SERIES Y/ZYZΔ CONNECTION

Series Y/ZYZΔ, $k_0 = 1$	
A	$[\frac{1}{\sqrt{3.27}} \frac{0.26}{\sqrt{3.27}} - (1 + \frac{3.73}{\sqrt{2}})]$
B	$[(1 + \frac{4L_p}{\sqrt{3.27}} - (1 + \frac{0.26}{\sqrt{3.27}})L_p + 3L_s - (1 + \frac{3.73}{\sqrt{3.27}})L_p + 3L_s)]$
C	$[\frac{3L_p}{\sqrt{3.27}} - ((1 + \frac{0.26}{\sqrt{3.27}})L_p + 4L_s) - (1 + \frac{0.26}{\sqrt{3.27}})L_p + 2L_s]$
D	$[1 + \frac{1}{\sqrt{3.27}} - (1 + \frac{1}{\sqrt{3.27}}) \frac{0.26}{\sqrt{3.27}} (1 + \frac{1}{\sqrt{3.27}})]$
E	$[-(1 + \frac{1}{\sqrt{3.27}} \frac{L_p}{4} + \frac{L_s}{4}) - (1 + \frac{1}{\sqrt{3.27}} \frac{L_p}{4}) 1 + \frac{L_p}{\sqrt{3.27}}]$
F	$[\frac{2.26L_p}{4\sqrt{3.27}} - (1 + \frac{1}{\sqrt{3.27}} \frac{L_p}{4} + \frac{3L_s}{4}) (1 + \frac{1}{\sqrt{3.27}} \frac{L_p}{4})]$
θ_1, θ_2	$\frac{9\pi}{24}, \frac{13\pi}{24}$
G, i	$0, i_r$

Figure 2 shows the NLAM of the circuit. The resistors in the model represent the overlap effects and the inductors are the coefficients of the first terms of the Taylor series of the load current.

$$\begin{aligned} V_{eq} &= \frac{12\sqrt{3.267}nVm}{\pi} \\ R_{eq} &= [\frac{12\omega n^2(0.82L_p + 0.36L_s)(3.267L_p + 0.27L_s)}{\pi} \left(0.36 + \frac{\sqrt{3.267}}{2} \right) + \\ &9.267n^2r_p \left(1 + \frac{\sqrt{3.267}}{2} \right) + 9.36n^2r_s + 9.36r_s] \\ L_{eq} &= \left[12.3 \left(0.36 + \frac{\sqrt{3.267}}{2} \right) n^2L_p + 2.36 \left(1.82 + \frac{\sqrt{3.267}}{2} \right) n^2L_p + 12L_s \right] \end{aligned} \quad (13)$$

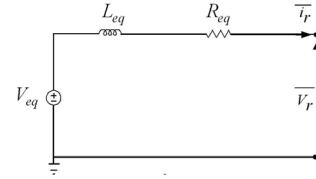


Fig. 2. Averaged value model of a series 24-pulse rectifier with Y/ZYZΔ transformer and constant power load

Figure (3) shows the detailed simulation of DC-link capacitor voltage and inductor current of a 24-pulse Y/ZYZΔ series-connected rectifier.

B. Parallel Y/ZYZΔ connection

When the three rectifiers are connected in a parallel (doubly-wound, transformer-based, 24-pulse rectifier), an IPR is required to support the instantaneous voltage difference in the three outputs. Figure 5 shows the diagram of the parallel, doubly-wound transformer-based, 24-pulse rectifier. The overall transformer turns ratio is again assumed to be $1 : n$.

Because of the IPR, the diode bridges will ideally, share the load current. Therefore, the constant k_0 in (11) has the value 0.25 and G in (11) is equal to L_{ipr} (The leakage inductance of the IPR). The expressions for the terms in equation (11) are listed in table III. Substituting these values into (11) will lead us to \overline{V}_r .

The expression for \overline{v}_r has the same form as (12) for the series connected rectifier, but with small differences.

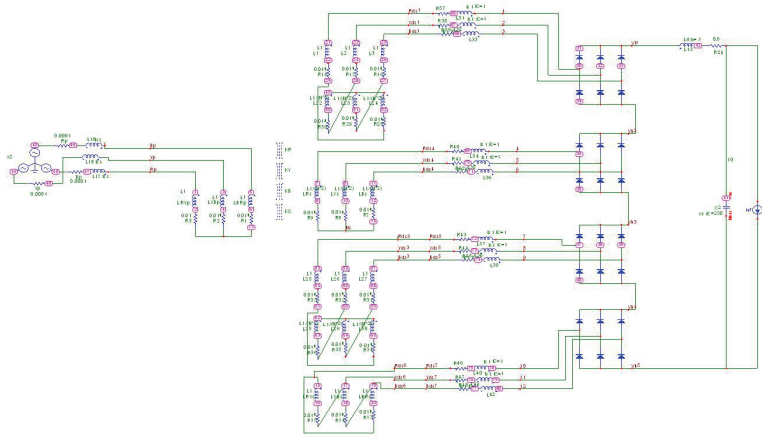


Fig. 4. A Series-connected output 24-pulse rectifier with an ideal Y/ZYZΔ transformer and constant power load

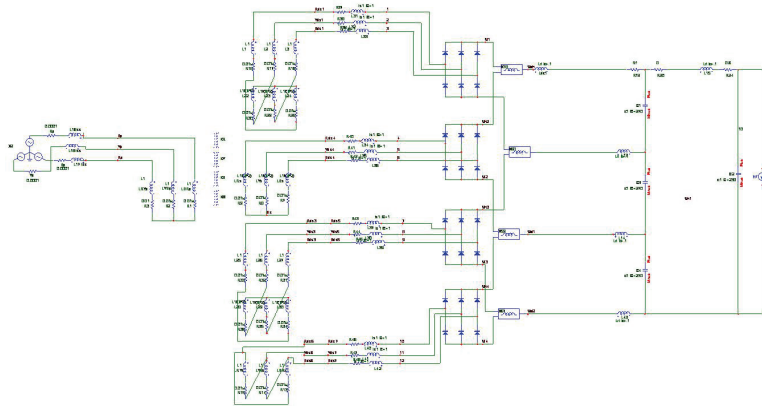


Fig. 5. A Parallel-connected output 24-pulse rectifier with an ideal Y/ZYZΔ transformer and constant power load

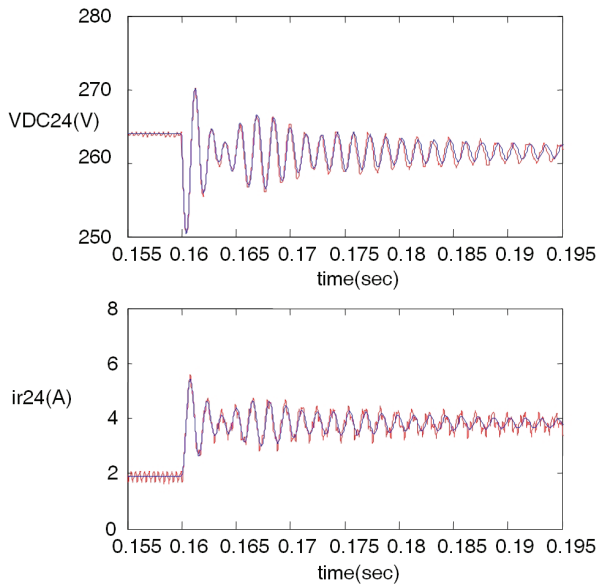


Fig. 3. Averaged value calculation and detailed simulation of DC-link capacitor voltage and inductor current of a 24-pulse Y/ZYZΔ series-connected rectifier using Micro-Cap 7 (detailed simulation (red), averaged model (blue))

TABLE III
REQUIRED PARAMETERS FOR PARALLEL Y/ZYZΔ CONNECTION

Parallel Y/ZYZΔ, $k_0 = 0.25$	
A	$[(1 + \frac{0.26\sqrt{3.267}}{4}) - 0.26(1 + \frac{1}{\sqrt{3.267}}) \frac{0.26(1 + \frac{3.73}{\sqrt{3.267}})]$
B	$[(1 + \frac{0.26}{\sqrt{3.267}}) \frac{L_p}{4} + \frac{L_s}{4} - (1 + \frac{0.26}{\sqrt{3.267}}) \frac{L_p}{4} (1 + \frac{L_p}{\sqrt{3.267}})]$
C	$[\frac{-3L_p}{4\sqrt{3.267}} - (1 + \frac{0.26}{\sqrt{3.267}}) \frac{L_p}{4} + \frac{3L_s}{4} - (1 + \frac{1}{\sqrt{3.267}}) \frac{L_p}{4}]$
E	$[1 + \frac{4L_p}{\sqrt{3.267}} (1 + \frac{0.26}{\sqrt{3.267}}) L_p + 3L_s - (1 + \frac{3.73}{\sqrt{3.267}}) L_p + 3L_s]$
F	$[\frac{-L_p}{\sqrt{3.267}} - (1 + \frac{L_p}{\sqrt{3.267}} + 4L_s) - (1 + \frac{L_p}{\sqrt{3.267}} + 2L_s)]$
θ_1, θ_2	$\frac{9\pi}{24} \quad \frac{13\pi}{24}$
G, i	$4L_{sr} \quad i_L/4$

$$\overline{V_r} = \frac{24\sqrt{3.267}nV_m}{2.2\pi} - \left(\frac{24\omega(n^2L_p + 3.267L_s)(0.36n^2L_p + 0.82L_s)}{2.2\pi} + (2.38n^2r_p(1 + \frac{\sqrt{3.267}}{2}) + 2.38r_s(1 + \frac{\sqrt{3.267}}{2}))\overline{i_r} - (2.37n^2L_p(0.38 + \frac{\sqrt{3.267}}{2}) + 2.38L_s(2 + \sqrt{3.267}) + 1.8L_{ipr})\frac{d\overline{i_r}}{dt} \right) \quad (14)$$

The parameters of the equivalent circuit are listed in (15).

$$V_{eq} = \frac{24\sqrt{3.267}nV_m}{2.2\pi} \quad (15)$$

$$R_{eq} = \frac{24\omega(n^2L_p + 3.267L_s)(0.36n^2L_p + 0.82L_s)}{2.2\pi} -$$

$$L_{eq} = \frac{(2.38n^2 r_p (1 + \frac{\sqrt{3.267}}{2}) + 2.38r_s (1 + \frac{\sqrt{3.267}}{2}))}{2} + 2.37n^2 L_p (0.38 + \frac{\sqrt{3.267}}{2}) + 2.38L_s (2 + \sqrt{3.267}) + 1.8L_{ipr}$$

Figure 6 shows the detailed simulation of DC-link capacitor voltage and inductor current of a 24-pulse $Y/ZYZ\Delta$ parallel-connected rectifier.

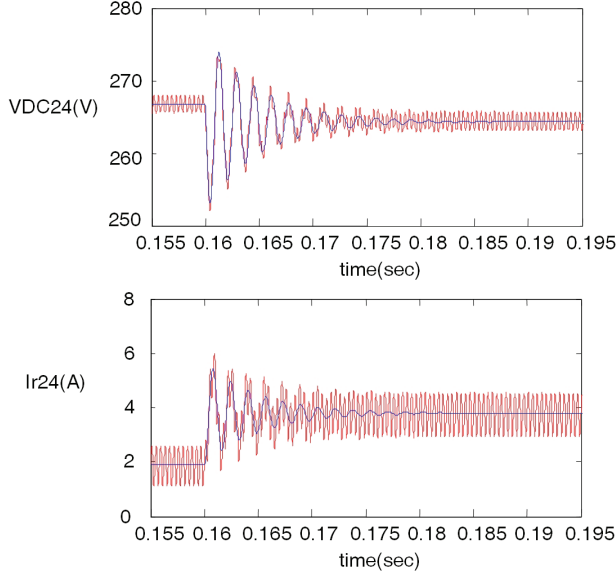


Fig. 6. Averaged value calculation and detailed simulation of DC-link capacitor voltage and inductor current of a 24-pulse $Y/ZYZ\Delta$ parallel-connected rectifier using Micro-Cap 7 (detailed simulation (red), averaged model (blue))

C. Autotransformer-based 24-pulse rectifier

Figure (7) shows a schematic diagram of an autotransformer based 24-pulse rectifier. The source voltages are according to 1. Every L_p is sum of the source inductance and transformer primary leakage inductances and every L_s represents an autotransformer secondary leakage inductance. The interphase reactors are modelled by two L_{sr} inductors, which represent the leakage inductances and an ideal autotransformer. The turn ratio of autotransformer is $k = 13.155$ to create required voltages for three phase bridges [1]. The method of averaging of this type of rectifier is similar to a $Y/ZYZ\Delta$ based 24-pulse rectifier. The output of every interphase reactor is the average of its input voltages. Therefore, the output voltage of the rectifier before the second order filter is according to 16.

$$\begin{aligned} \overline{V_r} &= \frac{24\sqrt{3.267}}{\pi} \sin(\frac{\pi}{24}) V_m + \frac{24\omega}{5\pi} (2.38(1 - \frac{6\sqrt{(3.267)}}{k}) L_p + \\ &+ 3.276(1 - \frac{6\sqrt{(3.267)}}{k}) L_s) \overline{i_r} \\ &- [4.3L_p + 2.38(1 - \frac{6\sqrt{(3.267)}}{k}) L_s + \frac{9}{2} L_{ipr}] \frac{di_r}{dt} - [\frac{9}{2} r_p + \frac{8}{3} r_s] \overline{i_r} \end{aligned} \quad (16)$$

Which means:

TABLE IV
REQUIRED PARAMETERS FOR AUTOTRANSFORMER CONNECTION

Autotransformer connection, $k_Q = 13.155$	
A	$[\frac{1}{2}(1 + \frac{1}{\sqrt{3.267}}) - \frac{3}{4}(1 + \frac{1}{0.267}) - (1 + \frac{1}{\sqrt{3.267}})]$
B	$[-(1 + \frac{1}{\sqrt{3.267}}) - ((1 + \frac{1}{\sqrt{3.267}}) L_p + \frac{3L_s}{4}) (1 + \frac{1}{0.267} L_p + \frac{3L_s}{4})]$
C	$[\frac{-4L_p}{\sqrt{3.267}} - ((1 + \frac{1}{0.267}) L_p + \frac{L_s}{2}) - ((1 + \frac{1}{0.267}) L_p + \frac{3L_s}{4})]$
D	$[(1 + \frac{4L_p}{\sqrt{3.267}}) (1 + \frac{0.267}{\sqrt{3.267}}) L_p + 3L_s - ((1 + \frac{3.73}{\sqrt{3.267}}) L_p + 3L_s)]$
E	$[-(1 + \frac{L_p}{4\sqrt{3.267}} + \frac{L_s}{4}) - (1 + \frac{L_p}{4\sqrt{3.267}}) ((1 + \frac{L_p}{\sqrt{3.267}})]$
F	$[\frac{3L_p}{4\sqrt{3.267}} - (1 + \frac{L_p}{4\sqrt{3.267}} + \frac{3L_s}{4}) (1 + \frac{1}{\sqrt{3.267}} \frac{L_p}{4})]$
θ_1, θ_2	$\frac{4\pi}{24} \quad \frac{11\pi}{24}$
G, i	$4L_{sr} \quad i_r/4$

$$\begin{aligned} V_{eq} &= \frac{24\sqrt{3.267}}{\pi} \sin(\frac{\pi}{24}) V_m \\ R_{eq} &= -\frac{24\omega}{5\pi} \left(2.38(1 - \frac{6\sqrt{(3.267)}}{k}) L_p + 3.276(1 - \frac{6\sqrt{(3.267)}}{k}) L_s \right) \\ &- \left[\frac{9}{2} r_p + \frac{8}{3} r_s \right] \\ L_{eq} &= - \left[4.3L_p + 2.38(1 - \frac{6\sqrt{(3.267)}}{k}) L_s + \frac{9}{2} L_{ipr} \right] \end{aligned} \quad (17)$$

Figure (8) shows the detailed simulation of DC-link capacitor voltage and inductor current of an Autotransformer based 24-pulse rectifier.

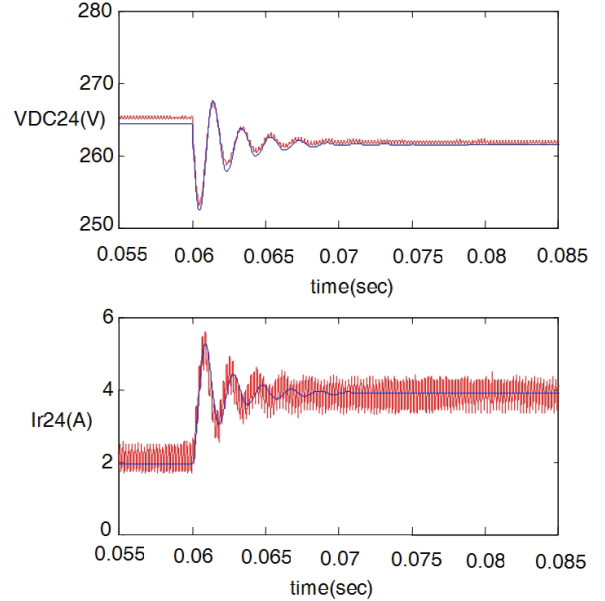


Fig. 8. Averaged value calculation and detailed simulation of DC-link capacitor voltage and inductor current of a 24-pulse Autotransformer-based rectifier using Micro-Cap 7 (detailed simulation (red), averaged model (blue))

IV. COMPARISON OF MODELS

Comparing the averaged models for the three transformer coupled rectifiers (Table II and Table III) it is seen that the no load voltage is doubled in the series-connected configuration for the same transformer turn ratio n , and the effects of the

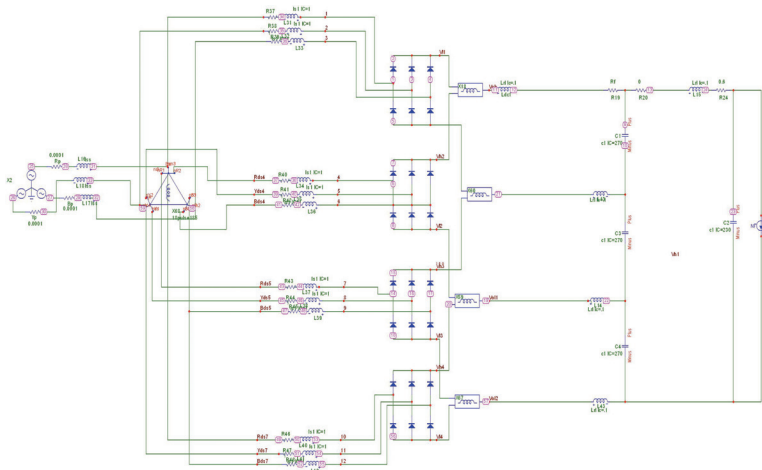


Fig. 7. Autotransformer based 24-pulse rectifier with a constant power load

primary and secondary inductances are four times larger. However, for the parallel-connected rectifier the leakage inductance of the *IPR* provides an additional series inductance in the equivalent circuit.

Comparing the averaged model of the three parallel connected rectifiers of Table III and Table IV; if the voltage ratio of the doubly-wound transformer n is set to unity, the no-load output voltages are slightly different, the voltage is $\frac{1}{\cos(\pi/24)}$ higher for the autotransformer-based system, which is the output-to-input voltage ratio of the autotransformer. Also, in the autotransformer-based circuit the values of the series inductance and overlap resistance terms are both $\frac{1}{\cos^2(\pi/24)}$ bigger than in the doubly-wound case. This suggests that the model for the autotransformer-based rectifier is a special case of parallel-connected rectifier model, with the turns ratio n set to $\frac{1}{\cos(\pi/24)}$. However, in next section it will be shown that there are important differences between the two rectifiers in terms of the way they interact in multi-rectifier systems. In addition the autotransformer-based system has increased output impedance due to the requirement for three inter-phase reactors.

V. CONCLUSION

DC-side, averaged-value models have been derived for three common 24-pulse rectifiers, the autotransformer configuration being of particular interest for size/weight critical applications such as in the more-electric aircraft. The models of the three rectifiers are seen to have strong similarities, for example the model of the autotransformer-based rectifier is seen to be a special case of the parallel-connected, 24-pulse rectifier with a transformer turns ratio of $\frac{1}{\cos(\pi/24)}$, however in addition a second *IPR* is required in the autotransformer circuit. The models have been validated by comparison with detailed simulations. It has also been seen that the individual equivalent circuit models may be straightforwardly coupled together to examine the behavior of systems that consist of multiple rectifiers of the same type. By means of this averaging method

the complexity of a rectifier based system model is reduced without any serious change in state space condition of the whole system. Therefore, this method of modelling can be very useful in analysis and design of a system with a number of rectifiers with high pulse conversion.

REFERENCES

- [1] S. Choi, P. N. Enjeti, I. J. Pitel, *Polyphase Transformer Arrangements with Reduced KVA Capacities for Harmonic Current Reduction in Rectifier-Type Utility Interface*, IEEE Transactions in power Electronics Vol. 11, No. 5, Sep. 1996, pp. 680–690.
- [2] J. T. Alt, S. D. Sudhoff, *Average Value Modelling of Finite Inertia Power System With Harmonic Distortion*, 2000 SAE Transactions, Journal of Aerospace, section 1, pp.932-946.
- [3] S. D. Sudhoff, O. Wasynczuk, *Analysis and Average Value Modelling of Line-Commutated Converter Synchronous Machine System*, IEEE Tran. on Energy Conversion, Vol.8, No.1, March 1993, pp. 92-99.
- [4] S. D. Sudhoff, *Waveform Reconstruction From The Average Value Model of line-Commutated Converter Synchronous Machine System*, IEEE Trans. on Energy Conversion, Vol. 8, No. 3, September 1993, pp.404-410.
- [5] S. D. Sudhoff, *Analysis and Average Value Modelling of Dual Line-Commutated Converter 6-phase Synchronous Machine Systems*, IEEE Tran. on Energy Conversion, Vol.8, No.3, September 1993, pp. 411-417.
- [6] A. Baghrarian, A. J. Forsyth, *Averaged-value models of twelve-pulse rectifiers for aerospace applications*, PEMD 2004, Vol. 1, pp. 220–225.
- [7] D. A. Paice, *Power Electronic Converter Harmonics, Multi-pulse Method for Clean Power*, IEEE press, Piscataway, NJ, 1996.
- [8] S. Aghighi;A. Baghrarian;R. E. Ebrahimi; *Averaged value analysis of 18-Pulse rectifiers for aerospace applications*, IEEE International Symposium on Industrial Electronics, ISIE'09, 5-8 July 2009, pp.1498 – 1503.
- [9] K. Furmanczyk, M. Stefanich, *Demonstration of very high power airborne AC to DC converter*, SAE Power System Conference, Reno, Nevada, Nov. 2-4, 2004.
- [10] F. J. Chivite-Zabalza, A. J. Forsyth, D. R. Trainer, *Analysis and practical evaluation of an 18-pulse rectifier for aerospace applications*, Proceedings of the Second International Conference on Power Electronics, Machines and Drives, 2004, vol 1. pp. 338-343.
- [11] K. Furmanczyk, M. Stefanich, *Demonstration of very high power airborne AC to DC converter*, SAE Power System Conference, Reno, Nevada, Nov. 2-4, 2004.
- [12] A. Cross;A. Baghrarian;A. Forsyth, *Approximate, average, dynamic models of uncontrolled rectifiers for aircraft applications*, IET Power Electronics, Vol. 2, Issue 4, July 2009, pp. 398 – 409.
- [13] A. Baghrarian, *Modeling and analysis of multi-pulse rectifier systems*, PhD Thesis 2006, University of Birmingham.